Coordinated Damping Control Design for Power System With Multiple Virtual Synchronous Generators Based on Prony Method

Zhao, Min; Yin, Hang; Xue, Ying; Zhang, Xiao-ping; Lan, Yuanliang

DOI:
10.1109/OAJPE.2021.3104755

Document Version
Publisher's PDF, also known as Version of record

Citation for published version (Harvard):
Zhao, M, Yin, H, Xue, Y, Zhang, X & Lan, Y 2021, 'Coordinated Damping Control Design for Power System With Multiple Virtual Synchronous Generators Based on Prony Method', *IEEE Open Access Journal of Power and Energy*, vol. 8, pp. 316-328. https://doi.org/10.1109/OAJPE.2021.3104755

IEEE Open Access Journal of Power and Energy

Received 1 April 2021; revised 23 June 2021; accepted 5 August 2021.
Date of publication 13 August 2021; date of current version 26 August 2021.

Digital Object Identifier 10.1109/OAJPE.2021.3104755

Coordinated Damping Control Design for Power System With Multiple Virtual Synchronous Generators Based on Prony Method

MIN ZHAO[1], HANG YIN[2], YING XUE[1] (Senior Member, IEEE), XIAO-PING ZHANG[1] (Fellow, IEEE), AND YUANLIANG LAN[2]

[1]Department of Electronic, Electrical and Systems Engineering, School of Engineering, University of Birmingham, Birmingham B15 2TT, U.K.
[2]Global Energy Interconnection Research Institute Europe GmbH (GEIRI Europe), Kant Strasse 162, 10623 Berlin, Germany
CORRESPONDING AUTHOR: X.-P. ZHANG (x.p.zhang@bham.ac.uk)

This work was supported in part by the Engineering and Physical Sciences Research Council (EPSRC) under Grant EP/N032888/ and Grant EP/L017725/1 and in part by Global Energy Interconnection Research Institute Europe GmbH under Grant SGRIKXWT-2017-270.

ABSTRACT With more renewables integrated into power grids, the systems are being transformed into low inertia power electronic dominated systems. In this situation, the virtual synchronous generator (VSG) control strategy was proposed to deal with insufficient inertia challenge caused by the reduction of synchronous generation. However, as the VSG control method emulates the dynamic behavior of traditional synchronous machines, the interaction between multiple VSG controllers and synchronous generators (SGs) may cause low-frequency oscillation similar to that caused by the interaction between multiple SGs. This paper reveals that the system low-frequency oscillatory modes are affected by multiple VSGs. Then Prony analysis is utilized to extract the system mode information which will be subsequently used for VSG controller design, and a decentralized sequential coordinated method is proposed to design the supplementary damping controller (SDC) for multiple VSGs. The system low-frequency oscillation is first analyzed based on a modified two-area system with a linearized state-space model, and a further case study based on a revised New England 10-machine 39-bus system is used to demonstrate the effectiveness of the proposed coordinated method for multiple VSGs.

INDEX TERMS Virtual synchronous generator (VSG), low-frequency oscillation, coordinated supplementary damping controller, decentralized control, sequential design method, Prony method, energy storage.

I. INTRODUCTION

OWING to the increasing penetration of power-electronic interfaced renewable energy sources, the current power system is transforming from synchronous generator (SG)-based structure to a power electronics-dominated one. This transformation poses significant challenges on system stability because of the reduced system inertia [1]. In order to address these challenges, the virtual synchronous generator (VSG) control with different implementation methodologies [2]–[6], [11], [16], [19], [20] was proposed and currently a VSG pilot project has been implemented in China [7]. The core of VSG is emulating the swing equation of SGs to provide virtual inertia support for power systems. The synchroverter concept was proposed in [2] which imitates both electrical and mechanical characteristics of SGs in stationary reference frame. It provides a clear and simple control structure to improve system frequency and voltage regulation capability. The power synchronization technique which enables the voltage-sourced converter (VSC) stations to behave like SGs was applied in [3]. Such control method improves the system stability for VSC-HVDC when connecting weak grid and therefore increases the transferred power. The inertia emulation control which utilizes the energy stored in the DC link capacitor was implemented [4] and it is equivalent to a virtual rotor. The emulated inertia enables the power electronic system to have better dynamic performance.

The virtual impedance [5] was introduced into VSG to enhance system controller flexibility. Apart from these, the VSG has also been enhanced from various aspects [8], [9] and it is proved to be a promising method to improve system stability.

Since VSG mimics the dynamic features of SGs, some inherent disadvantages such as power oscillations are also introduced by implementing such control strategy [6], [14]. The power oscillation is prone to occurring during load transients between VSG and SG devices due to inertia difference [12]. It was reported in [10] that the system suffers from undamped low-frequency oscillation instability because of the considerable grid resistance and the undesired coupling between active power and reactive power. [13] explained the resonance instability among parallel operated VSG and SG in the vicinity of natural frequency and stated that it is caused by the combination of governor and inertia characteristics.

However, most of the existing studies are mainly focused on the micro-grid systems. On the other hand, low-frequency oscillation is one of the major concerns for large power systems [14] especially under bulk power transfer between weakly connected power grids. Generally, there are several proposed methods to suppress the system power oscillation. The adjustment of VSG internal control parameters such as inertia and damping/droop coefficients are investigated in [10], [15] to improve system damping performance. However, it is also described that adjusting such parameters have limited impacts on system oscillation damping [17] and smaller inertia constant or larger damping coefficients can even degrade system behavior [6], [18], [21]. The virtual reactance was introduced to improve the system damping characteristics [22] while it may lead to reactive power calculation error [18].

In addition, some other methods were also proposed by employing additional stabilizing signal into the active power loop or reactive power/voltage loop to improve system damping [21], [23]–[25]. An improved damping control by modifying the voltage magnitude loop was introduced to VSG [21]. [24] proposed a strategy which implements a combination of power feedback signal and the derivative of virtual frequency feedback signal into the active power loop to enhance the damping of VSG. Similarly, the application of identification-based hierarchical control was investigated in [23] and this supplementary signal was also added into the real power loop. However, considering the potential risk of introducing torsional oscillation when injecting supplementary signal into the active power loop if the prime mover power of VSG comes from wind turbines [26], the additional damping signal is applied to the reactive power loop in this paper. Furthermore, as the virtual excitation control is implemented, the proposed supplementary control in this paper is added to the voltage droop loop rather than directly regulating the internal voltage magnitude as discussed in [21]. The proposed supplementary control in this paper is similar to the power system stabilizer (PSS)-based control, which can provide one more degree of freedom to enhance the system damping performance and it is easy to be implemented in practice.

The coordinated damping control for multiple VSGs is particularly useful to reduce the undesired coupling between them and also increase the damping of multiple dominant system oscillation modes. Generally, the coordinated control can be categorized into a multi-input-multi-output (MIMO) centralized control or a decentralized control [27] which usually decouples the system into multiple loops of single-input-single-output (SISO) one. Re-organizing a MIMO control problem into SISO control issue makes it more viable and attractive for practical power system. Besides, the centralized control is highly dependent on communication, therefore, it increases the system investment, the system control complexity and decreases the system reliability when there is a loss of communication [28]. The communication-less decentralized coordination control with a local structure is therefore more preferable. The sequential approach is generally implemented to design the controllers for a group of devices. A series of coordinated controllers for multiple FACTS devices are designed and studied with sequential strategy in [29]. Similarly, the sequential design method is utilized to ensure the multiple damping controllers of VSGs to work cooperatively.

In the past, Prony method [30] was utilized to extract the system oscillatory modes information since it is complex and unrealistic for practical large-scale power grid to obtain required system oscillation behavior using conventional modal analysis. Hence, in this paper, Prony method will be applied along with the coordinated sequential design approach for power systems with multiple VSGs. To the best knowledge of the author, there was limited research work on the coordinated control design of power systems with multiple VSGs. The main contributions of the paper can be summarized as below,

(1) The impact of multiple VSGs on system low-frequency oscillation is investigated and it is revealed that the VSGs are involved in the low-frequency oscillation modes (both local and inter-area modes). The virtual phase angle and angular frequency (θ_{vir} and ω_{vir}) participate in related modes significantly;
(2) The Prony analysis is applied for multiple VSGs supplementary damping controller (SDC) design. It is used to extract the low frequency modes information. Such measurement-based analysis provides more feasible and flexible design approach for SDC;
(3) A coordinated supplementary controller is designed for the virtual exciter loop to provide additional damping. The decentralized sequential control technique is employed to coordinate the supplementary controller design for multiple VSGs. The designed controller is easy to implement and can suppress the system low-frequency oscillation effectively.

The rest of the paper is organized as follows. The VSG control strategy which emulates the SG's characteristics is

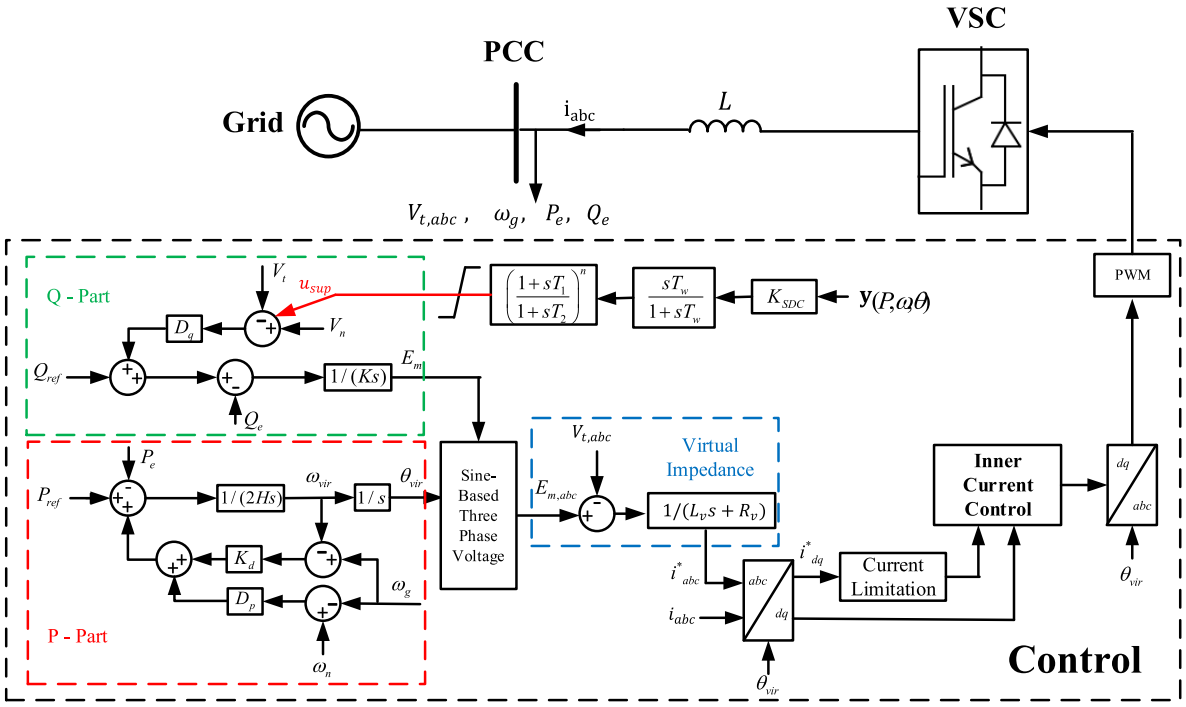

FIGURE 1. **Diagram of VSG control.**

briefly described in Section II. The commonly used two system oscillation identification methods are reviewed in Section III. Section IV describes the proposed decentralized coordinated sequential control strategy. The analytical results of the revised two-area system with multiple VSGs are presented and the time-domain simulation with the designed controller is studied in Section V. A revised New England 39-bus system is also investigated in this Section. Section VI draws the conclusion.

II. VIRTUAL SYNCHRONOUS CONTROL STRATEGY

The operating principle of VSG control scheme, which typically has energy storage capability, is described briefly in this section and the control structure is shown in Fig.1. (The variables in this figure are based on per unit system if not specified)

A. ACTIVE POWER CONTROL (P-PART)

The active power part (P-Part in Fig. 1) is the core of VSG which emulates the virtual inertia, damping and droop function.

The rotor equation and $P-f$ droop equation can be expressed as:

$$\begin{cases} 2H\dfrac{d\omega_{vir}}{dt} = P_m - P_e + K_d\left(\omega_g - \omega_{vir}\right) \\ P_m = P_{ref} + D_p\left(\omega_n - \omega_g\right) \\ \dfrac{d\theta_{vir}}{dt} = \omega_b\omega_{vir} \end{cases} \tag{1}$$

where P_m, P_e and P_{ref} are the virtual prime mover power, the converter output active power and reference; H, K_d and D_p are the virtual inertia constant, virtual damping coefficient and virtual $P-f$ droop coefficient; ω_b, ω_n, ω_g and ω_{vir} are the base frequency, nominal frequency, measured system frequency and generated virtual angular frequency; and θ_{vir} is the virtual phase angle.

B. REACTIVE POWER CONTROL (Q-PART)

For the reactive power part (Q- Part in Fig. 1), the virtual excitation control can provide a better transient performance [31] and therefore it is used to generate required voltage magnitude. The designed SDC is also introduced in this part.

$$E_m = G_{ex}(s)\left(V_{ref} - V_t + u_{sup}\right) \tag{2}$$

where V_{ref}, V_t and E_m are voltage reference, measured voltage at point of common coupling (PCC) of system and generated virtual voltage magnitude, u_{sup} is the supplementary signal and $G_{ex}(s)$ is the virtual excitation transfer function.

If V_t can track the reference value without static error, then an integration block should be included in $G_{ex}(s)$. If the $V-Q$ droop is considered as well:

$$V_{ref} = V_n + (Q_{ref} - Q_e)/D_q \tag{3}$$

where Q_e and Q_{ref} are the converter output reactive power and reference, V_n is the nominal voltage and D_q is the droop coefficient. Combining (2) and (3) together, the following can

be developed:

$$E_m = \frac{G_{ex}(s)\left(D_q\left(V_n - V_t + u_{sup}\right) + \left(Q_{ref} - Q_e\right)\right)}{D_q} \quad (4)$$

If $\frac{G_{ex}(s)}{D_q} = \frac{1}{Ks}$ (4) is expressed as:

$$K\frac{dE_m}{dt} = D_q\left(V_n - V_t + u_{sup}\right) + \left(Q_{ref} - Q_e\right) \quad (5)$$

where K is the virtual excitation coefficient.

C. VIRTUAL IMPEDANCE

The virtual impedance is adopted to facilitate the implementation of inner current loop [32],

$$i^*_{abc} = \frac{E_{m,abc} - V_{t,abc}}{(L_v s + R_v)} \quad (6)$$

where i^*_{abc}, $E_{m,abc}$ and $V_{t,abc}$ are the generated current reference, virtual voltage and measured voltage in *abc* stationary reference frame, L_v and R_v are the virtual inductance and virtual resistance. The current limitation [33] is also considered to guarantee the secure operation of converters.

III. OSCILLATION MODE IDENTIFICATION METHODS

The commonly used two system oscillation identification methodologies, i.e., the modal analysis and Prony method are briefly reviewed in this section.

A. MODAL ANALYSIS

The modal analysis is dependent on the detailed system modelling and system components are introduced respectively as below.

1) SYNCHRONOUS GENERATOR

The six-order model of synchronous generator and the IEEE type-1 excitation system are modelled [34].

2) VIRTUAL SYNCHRONOUS GENERATOR (VSG)

The mathematical modelling of VSG control is described in Section II. It should be mentioned that the VSG equations are derived under local *dq*-reference frame, therefore, it is necessary to transform physical quantities in the local *dq*-reference frame to that in the unified system *DQ*-reference frame.

3) OVERALL SYSTEM

Combining all the system differential equations above and the power flow algebraic equations, the small-signal model of overall system is obtained by linearizing the equations at a specific operating point [35]. The system oscillation modes can be determined via eigenvalue analysis.

B. PRONY METHOD

The aforementioned modal analysis is subjected to the system modelling details and operating points, which may not be suitable for practical large-scale power systems. On the other hand, a measurement-based methodology, i.e., Prony analysis, which does not require detailed system information, is used in this paper to estimate the system modal features. Prony analysis constructs the signal with a set of complex functions [36],

$$\hat{y}_n = \sum_{i=1}^{p} M_i e^{j\theta_i} e^{(\alpha_i + j2\pi f_i)T_s n} = \sum_{i=1}^{p} H_i e^{\lambda_i t} \quad (7)$$

where $\hat{y}_n$ is an estimated signal of a data sequence $\hat{\boldsymbol{y}} = [\hat{y}_0, \hat{y}_1 \ldots \hat{y}_{N-1}]$, p is the order of the fitting model, M_i is the magnitude of i_{th} mode, θ_i is the phase angle, α_i is the damping coefficient, f_i is the frequency, T_s is the time interval of sampling and H_i is the i_{th} output residue including the input signal (rather than the transfer function residue).

Considering that the system is represented in Laplace domain ($Y(s) = G(s)U(s)$), the transfer function can be represented in residue form as:

$$G(s) = \sum_{i=1}^{p} \frac{R_i}{s - \lambda_i} \quad (8)$$

The residue H_i contains the input signal information, which is not specified in (7). If input $U(s)$ is given and it is assumed as a step signal, then the transfer function residue can be calculated as [30]:

$$\begin{cases} U(s) = \sum_{i=0}^{k} c_i \dfrac{e^{-sD_i} - e^{-sD_{i+1}}}{s} \\ R_j = \dfrac{H_j \lambda_j}{\sum_{i=0}^{k} c_i e^{\lambda_j (D_k - D_i)}} j = 1, 2 \ldots p \end{cases} \quad (9)$$

After applying a known input disturbance to the power system and then performing the Prony analysis using the corresponding output, the transfer function residue can be obtained. The estimated system information from Prony method can be used to guide the system controller design.

IV. DECENTRALIZED COORDINATED SEQUENTIAL DAMPING CONTROLLER DESIGN

In this part, a decentralized coordinated sequential design approach for the system with multiple VSGs is presented. The proposed scheme is based on identified system transfer function with Prony method. A general description is demonstrated in this Section.

In order to obtain the identified model, a probing signal is injected to VSG (e.g., a step voltage reference with small magnitude is applied to the VSG Q-part loop) as shown in Fig. 2, the corresponding output related to the power oscillation such as the active power and virtual angular frequency, etc., is used to extract the system oscillatory modes using Prony method. The obtained oscillatory pattern is then utilized to develop a reduced-order model for the system.

The structure of SDC is depicted in Fig. 1 where y is the selected feedback signal from the VSG. K_{SDC} is the supplementary controller gain; T_w is the time constant of the wash-out block and its typical values are 1∼20s [35] and it is set to 3s in this paper; T_1 and T_2 are the time constants of the lead-lag block. After obtaining the system oscillatory

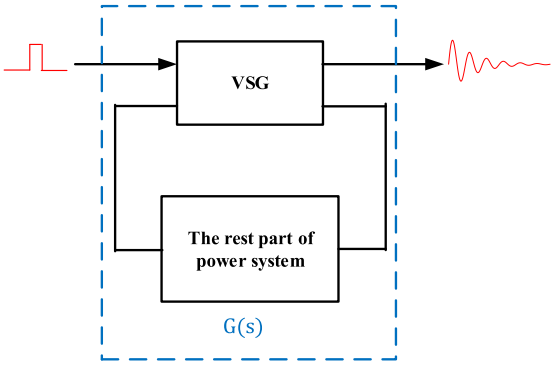

FIGURE 2. **Data sampling process.**

information, the residue method is utilized to calculate the lead-lag block parameters. With the identified system transfer function $G(s)$ and the obtained SDC parameters, K_{SDC} can be determined with root-locus method.

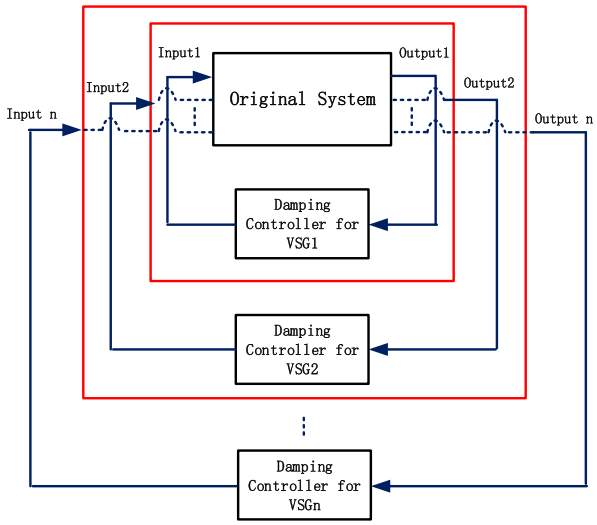

FIGURE 3. **Sequential design approach.**

To coordinate the damping controllers for multiple VSGs, the sequential approach depicted in Fig. 3 is implemented. The power grid is first treated as a SISO system and the damping controller for the first VSG is designed with preceding steps. After obtaining the damping controller for first VSG, the closed-loop system model including the designed controller is formed (as highlighted in Fig. 3) and it is regarded as a new open-loop system for the next VSG damping controller design. With such method, undesired adverse interactions among the different VSG units in damping controller design can be reduced and the design process of multiple damping controllers can be simplified as well.

The complete controller design process can be summarized as following,

(1) Step 1: Injecting a specified control input disturbance to the first VSG and extracting the system oscillatory information with Prony method;
(2) Step 2: Designing the damping controller with obtained system information and testing the system performance. More specifically, the parameters of lead-lag block are obtained based on residue method and the stabilizing gain is determined with root -locus method;
(3) Step 3: Repeating Step 1 and Step 2 to design damping controller for next VSG;
(4) Step 4: Validating the effectiveness of designed controller after finishing the decentralized sequential damping controller for multiple VSGs.

V. STABILITY ANALYSIS AND SIMULATION RESULTS

In this section, a revised two-area system is first analyzed with both modal analysis and Prony method, a decentralized sequential control method is then proposed for the damping controller design of multiple VSGs. A more complex power system is studied as well to confirm the effectiveness of designed controller. The simulation results are based on phasor-type model in MATLAB/Simulink.

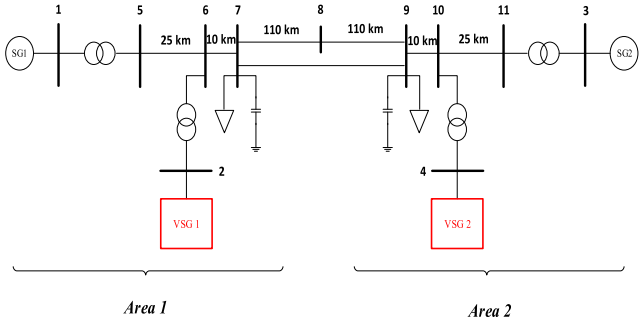

FIGURE 4. **Single-line diagram of modified two-area system.**

A. MODAL ANALYSIS, CONTROLLER DESIGN AND SIMULATION OF TWO-AREA SYSTEM

A modified case based on the two-area benchmark system [35] is used to analyze the impact of VSGs on power systems low-frequency oscillation. The system topology is depicted in Fig. 4. Two VSGs are employed to replace the SGs in bus 2 and bus 4 respectively. Both VSGs are producing the same active power as the original SGs to maintain the power balance. The PSSs of SGs are deactivated to facilitate a clear demonstration about the impacts of VSGs. Most system parameters can be found in [35] and the detailed parameters of VSG controller are listed in Table 3.

1) ELECTRO-MECHANICAL STABILITY ANALYSIS

The low-frequency oscillation patterns of the two-area system are obtained by applying modal analysis and the results are shown in Table 1. As can be seen from Table 1, there are three low-frequency oscillation modes of the modified two-area system. Theoretically, there will be $n-1$ low frequency oscillatory modes if n swing equations are included in the system. As there are two SGs and two VSGs, four rotor dynamic equations lead to three low-frequency oscillation

TABLE 1. Eigenvalue analysis results of revised two-area system.

No.	Frequency (Hz)	Damping ratio	Dominant states
1	1.167	0.101	$\omega_{SG2}, \theta_{SG2}; \omega_{VSG2}, \theta_{VSG2}$
2	1.137	0.116	$\omega_{SG1}, \theta_{SG1}; \omega_{VSG1}, \theta_{VSG1}$
3	0.588	0.056	$\omega_{SG1}, \theta_{SG1}; \omega_{SG2}, \theta_{SG2};$ $\omega_{VSG1}, \theta_{VSG1}; \omega_{VSG2}, \theta_{VSG2}$

modes, one inter-area mode and two local modes which is similar to that of the original two-area benchmark system.

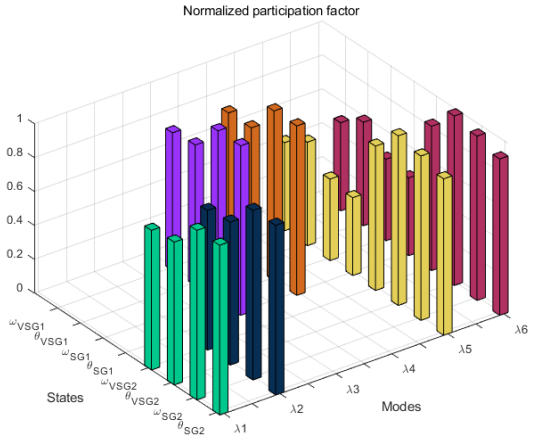

FIGURE 5. Normalized participation factor for low-frequency modes.

The normalized participation factors [34] for three modes are presented in Fig. 5. For the conjugate eigenvalues λ_1 and λ_2, they are related to mode 1 and high participation factor values of related states (θ_{SG2}, ω_{SG2}, θ_{VSG2} *and* ω_{VSG2}) reveal that they are dominant in this local oscillation. Similarly, λ_3 to λ_6 show that virtual swing equation states (θ_{VSG}, ω_{VSG}) have a considerable interaction with the SG rotor states (θ_{SG}, ω_{SG}).

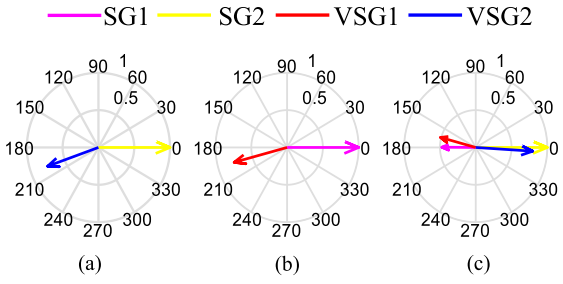

FIGURE 6. Mode shapes. (a) mode1; (b) mode 2; (c) mode 3.

The calculated mode shapes related to the three low-frequency modes are illustrated in Fig. 6. Fig. 6(a) and (b) demonstrate the mode shapes of local modes where SG2 oscillates against VSG2 in area 2 and SG1 oscillates against VSG1 in area 1. For mode 3, it is obvious that the VSG and SG group in area 1 are oscillating against the other group in area 2. Traditionally, the homogenous generators in the same area are determined based on geographical locations and the different areas are usually linked with weak tie-lines [35]. From these results, it can be observed that the integration of VSGs into the power grid has similar effects on system low-frequency oscillation modes like SGs.

2) SEQUENTIAL SUPPLEMENTARY DAMPING CONTROLLER FOR MULTIPLE VSGs

Based on the previous analysis, the VSGs have strong interactions with SGs in low-frequency range. In order to suppress such oscillation mode, the aforementioned coordinated decentralized sequential damping control is implemented.

Normally, the variables related to the power oscillation are considered as candidates for feedback signals. In this paper, the VSG active power output is chosen as feedback input signal for the auxiliary damping controller. The supplementary signal is added in the virtual excitation loop because additional modulation in active power loop may introduce mechanical vibrations and will shorten the lifespan of mechanical structures if they are applied to wind system [37]. As the feedback signal is extracted from the local signal, the time compensation caused by the communication delay is not considered.

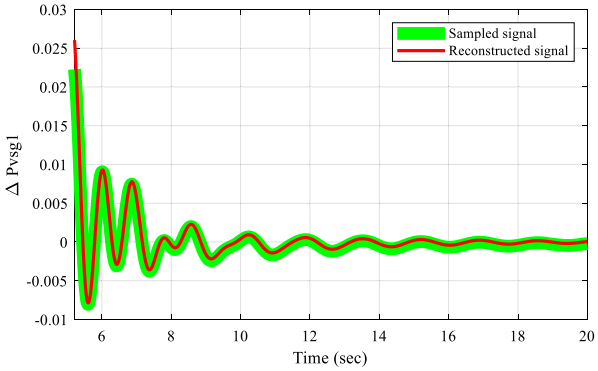

FIGURE 7. Reconstructed signal.

Before implementing the Prony method, a step input is injected to VSG1 to obtain the transfer functions. The step change of V_n is applied to the Q-part of VSG1 and the active power of $P_{e,VSG1}$, is chosen as the output signal, which will then be used for the Prony analysis. As can be observed in Fig. 7, the reconstructed signal in red approximates the actual signal well. The estimated low-frequency mode information is listed in Table 2. The first two modes reveal that the VSG1 has a high participation in such oscillation and this is consistent with the eigenvalue analysis in Table 1. The mode (1.167 Hz) is not identified as VSG1 is not participated in it.

From the extracted results based on Prony analysis, a reduced-order system transfer function can be obtained. The bode plot as shown in Fig. 8 shows that it has a relatively good fitness in the frequency range of interest.

The obtained residue information in Table 2 is utilized to calculate the parameters of lead-lag block. Although mode 2 with large residue is chosen for the calculation, the damping

TABLE 2. Identified reduced-order system transfer function.

Mode	Frequency (Hz)	Damping ratio	Eigenvalue	Residue (R∠ϕ)
1	0.593	0.058	$-0.217 \pm j3.726$	$0.186\angle 2.95^o$
2	1.148	0.112	$-0.813 \pm j7.213$	$0.991\angle -24.03^o$
3	0	--	-0.00123	$-0.0133\angle 180^o$
4	0	--	-0.325	$-0.119\angle 180^o$
5	0	--	-0.974	$0.854\angle 0^o$
6	0	--	-1.551	$0.342\angle 180^o$

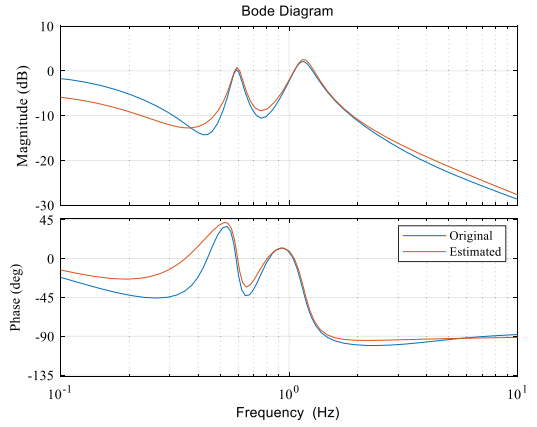

FIGURE 8. Bode plot.

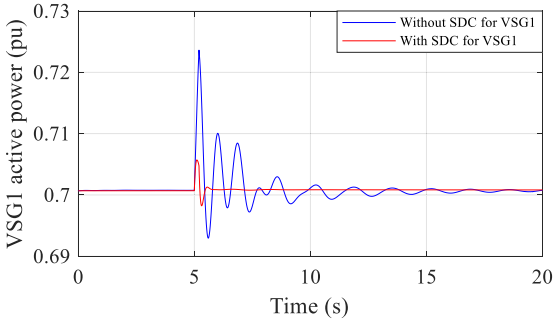

FIGURE 9. Active power response under V_n disturbance.

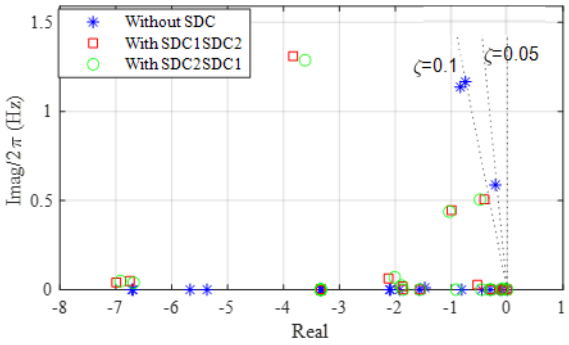

FIGURE 10. System damping with designed coordinated controller.

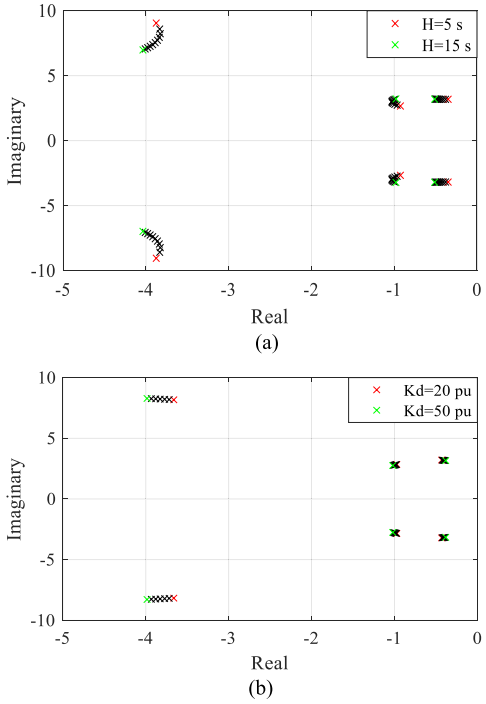

FIGURE 11. Impact of different virtual inertia and damping with designed controller.

of other modes will be increased if possible. The supplementary controller gain K_{SDC} for VSG1 is determined using root-locus method with identified system transfer function. The simulation shown in Fig. 9 verifies the effectiveness of the designed controller for VSG1 with a step disturbance in V_n.

As there are multiple VSGs in the test system, the supplementary controller for each VSG should be designed in a coordinated manner. Using the sequential coordination method described in Section IV, the controller is designed step by step, i.e., SDC1 for VSG1 and then SDC2 for VSG2. As the dynamics of SDC1 are already incorporated into the Prony analysis for SDC2 design, the coordination of the multiple supplementary controllers can be achieved. It should be mentioned that different design sequence may lead to different controllers, but it has small effect on the overall system damping performance [29]. The damping with different design sequences is compared in Fig. 10 where SDC1SDC2 represents design of the VSG1 first and then VSG2, SDC2SDC1 represents the reversed sequence. It shows that the overall system damping is almost the same with different design sequences.

With the designed controller, the analysis of the impact of different virtual inertia and damping coefficients on the system eigenvalues is presented in Fig. 11. it can be seen that higher H shifts the three modes towards left within the varied range (5∼15s) which indicates that the designed scheme can achieve satisfactory performance with high virtual inertia of

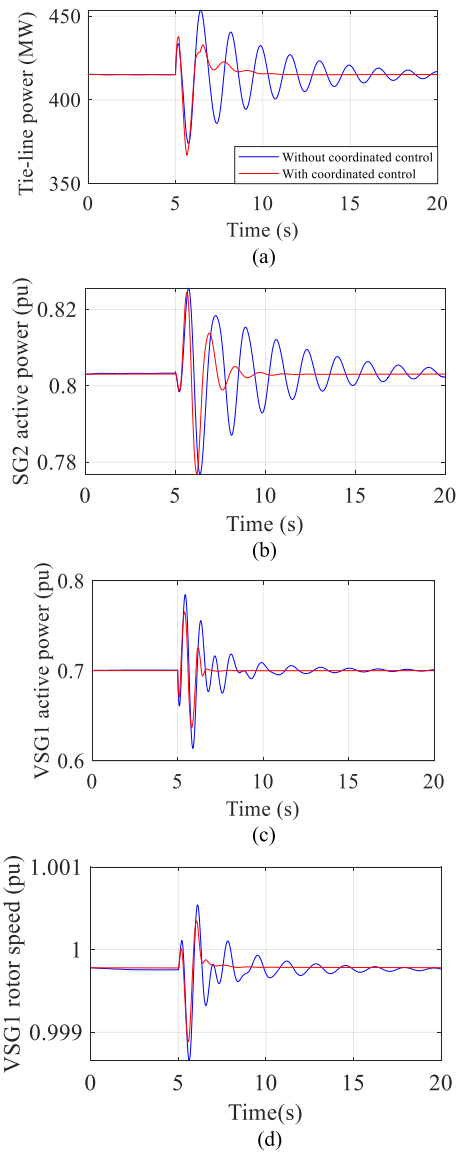

FIGURE 12. **Two-area system response under generator excitation disturbance.**

VSG. When the virtual damping K_d changes from 20 *pu* to 50 *pu*, it can be seen that there are limited impacts on the two modes near the imaginary axis, while it makes the mode with higher frequency to move towards left. Therefore, it can be inferred that the designed scheme is robust to a varied range of virtual inertia and damping coefficients of VSGs.

3) TIME-DOMAIN SIMULATION

In order to validate the effectiveness of the designed coordinated damping controllers, simulation studies of a step excitation disturbance and a three-phase-to-ground fault are carried out on the 11-bus two-area system.

A step disturbance lasting 0.2s with 0.05 *pu* magnitude is applied to the excitation control of SG1, the system responses are illustrated in Fig.12. It can be found from Fig. 12(a) to (d)

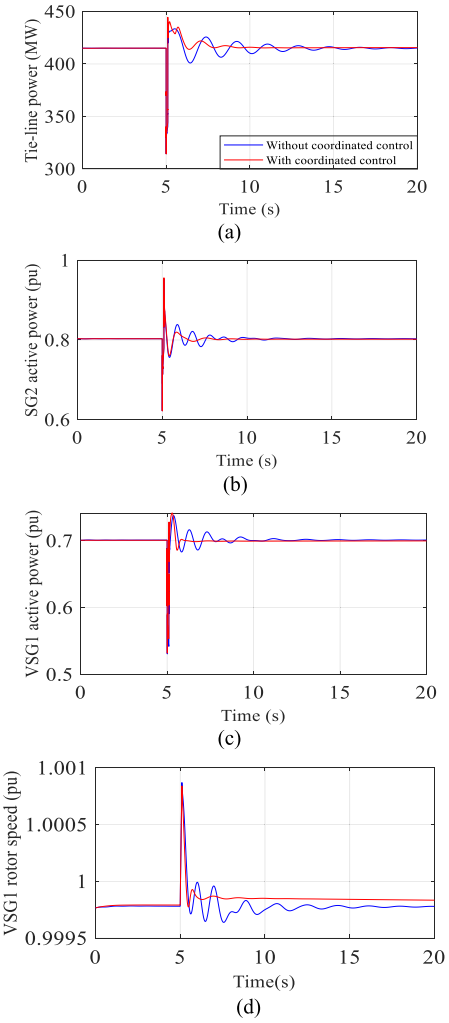

FIGURE 13. **Two-area system response under fault disturbance.**

that the designed controller can improve system damping. The tie-line power oscillation as shown in Fig. 12(a) is suppressed considerably with the proposed coordinated controller. The active power oscillation of SG2 as shown in Fig. 12(b) is damped quickly with the designed controller. Besides, the rotor speed and active power of VSG1 have better damping performance.

In addition, the effectiveness of the coordinated damping controller is verified by simulating a three-phase-to-ground fault on one of the transmission lines between two areas at 5s with a duration of 0.1s. The simulation results are shown in Fig. 13. It can be observed that the designed controllers are very helpful to system oscillation suppression. It enhances the system damping performance under fault disturbance.

Another four cases (case 3 to case 6) are also simulated to validate the robustness of designed controller. The same three-phase-to-ground fault is applied to these cases except Case 4.

Case 3: The impact of heavily loaded tie-line. The 300MW load in area 1 is transferred to area 2 which changes the power flow through the tie-line from 413MW to 670MW.

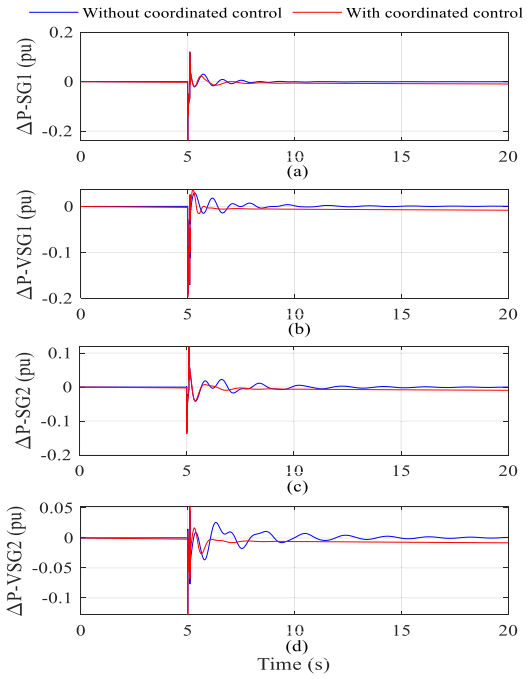

FIGURE 14. Two-area system simulation for heavily loaded tie-line.

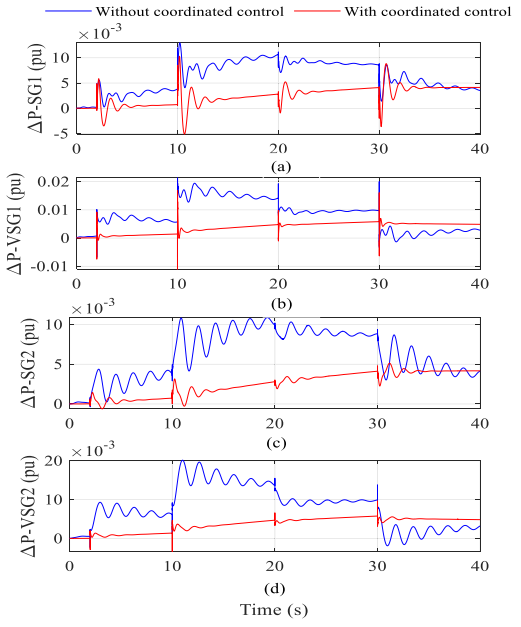

FIGURE 15. Two-area system simulation for continuously changing load.

Case 4: The impact of continuously changing load. A 15MW load is added to bus 7 at 2s, following by 25MW load increase at 10s, a decrease of 10MW load at 20s and a further 20 MW decrease at 30s.

Case 5: The impact of electrical distance of tie-line. The distance of the tie-line between two areas are set as 180km, 220km and 260km respectively.

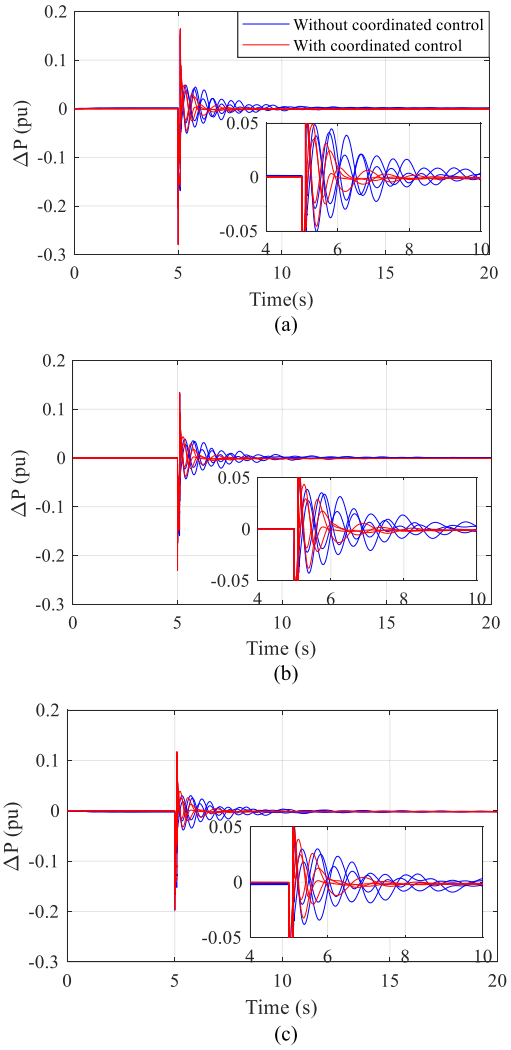

FIGURE 16. Two-area system simulation for different electrical distance. (a) 180 km. (b) 220 km. (c) 260 km.

Case 6: The impact of penetration level of VSG. The SG1 in the two-area system is replaced with a new VSG to model 3VSGs system. An all-VSGs system is further developed by replacing SG2 with a VSG. Therefore, the system studies with non-synchronous generation levels of 50%, 75% and 100%, respectively, are carried out.

The simulation results of case 3 and case 4 are shown in Fig. 14 and Fig. 15. It can be observed that the oscillation of four sources (SGs and VSGs) with designed scheme is suppressed quickly than that without the proposed control. The active power from all devices is plotted in Fig. 16 and Fig. 17 to show the simulation results of case 5 and case 6. The effective damping of power oscillations demonstrates the system damping improvement when using the proposed method.

B. TEST RESULTS ON THE 39-BUS SYSTEM

To further validate the performance of the proposed method in a more complex power system, a modified New England

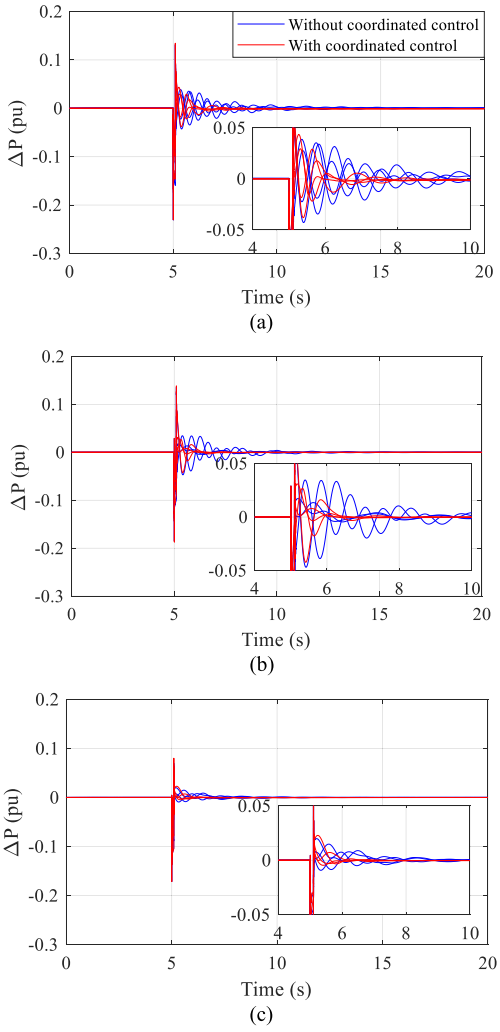

FIGURE 17. Two-area system simulation for different penetration level. (a) 50% km. (b) 75%. (c) 100%.

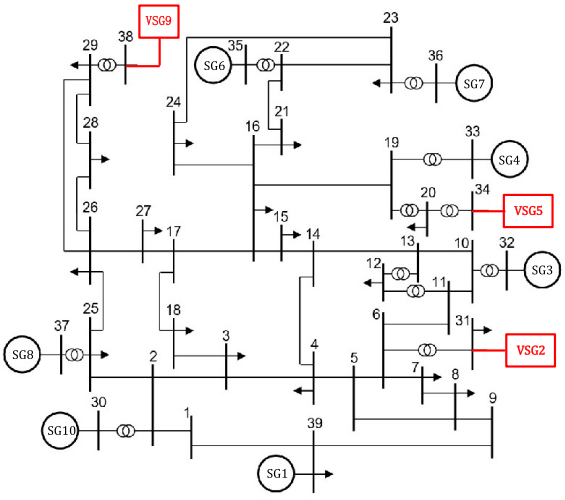

FIGURE 18. Modified new England 39-bus system.

system depicted in Fig. 18 is developed. The detailed system parameters can be found in [38]. In this system, SG2, SG5 and

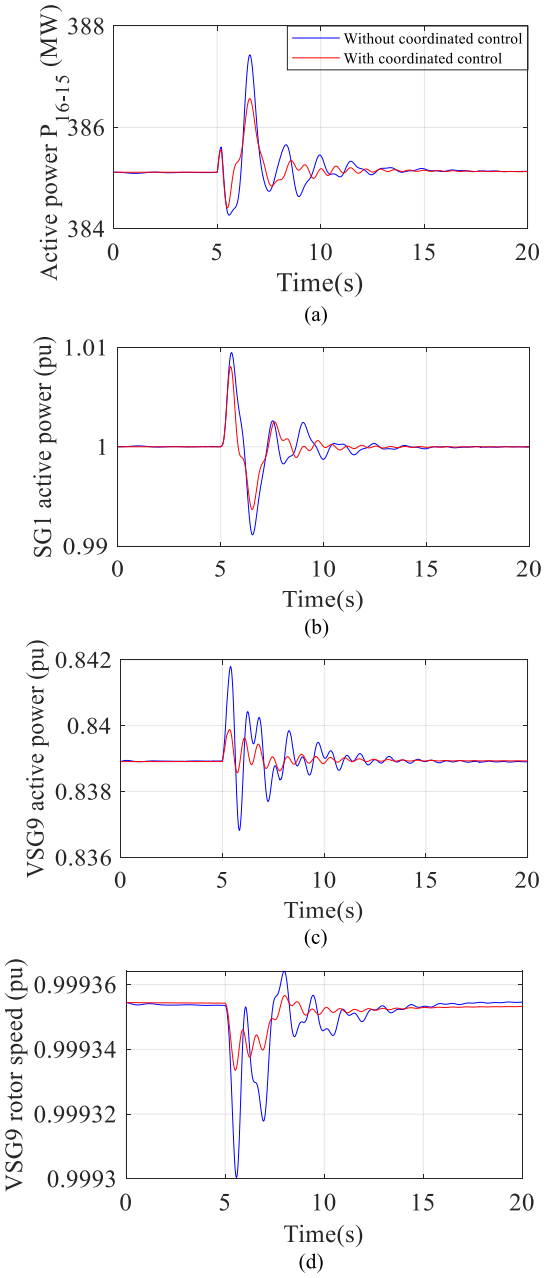

FIGURE 19. 39-bus system response under generator excitation disturbance.

SG9 are replaced with three VSGs. PSSs are activated for the remaining synchronous generators except SG1. The supplementary controller is first designed for VSG2 and followed by VSG5 and VSG9. Three different disturbances are used to validate the effectiveness of designed controller and the time-domain simulation results are shown as below.

1) SYNCHRONOUS GENERATOR DISTURBANCE

A step disturbance with 0.05 *pu* amplitude is applied to the excitation voltage reference of SG10 for 0.2s. The active power of SG1, the power flow on Line 15-16, the rotor speed

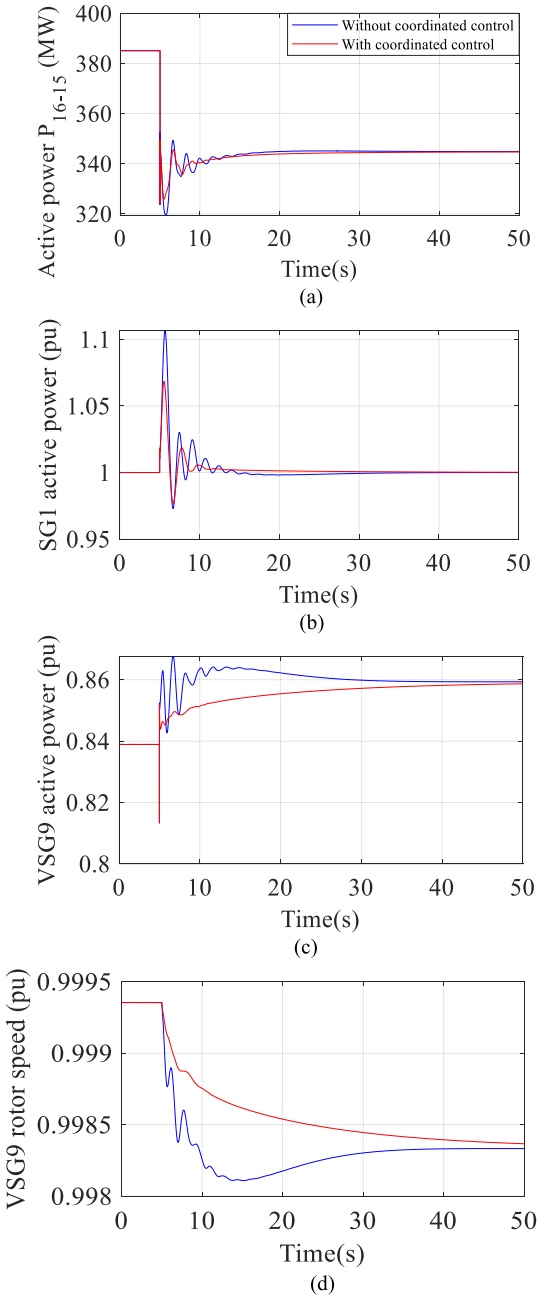

FIGURE 20. **39-bus system response under load disturbance.**

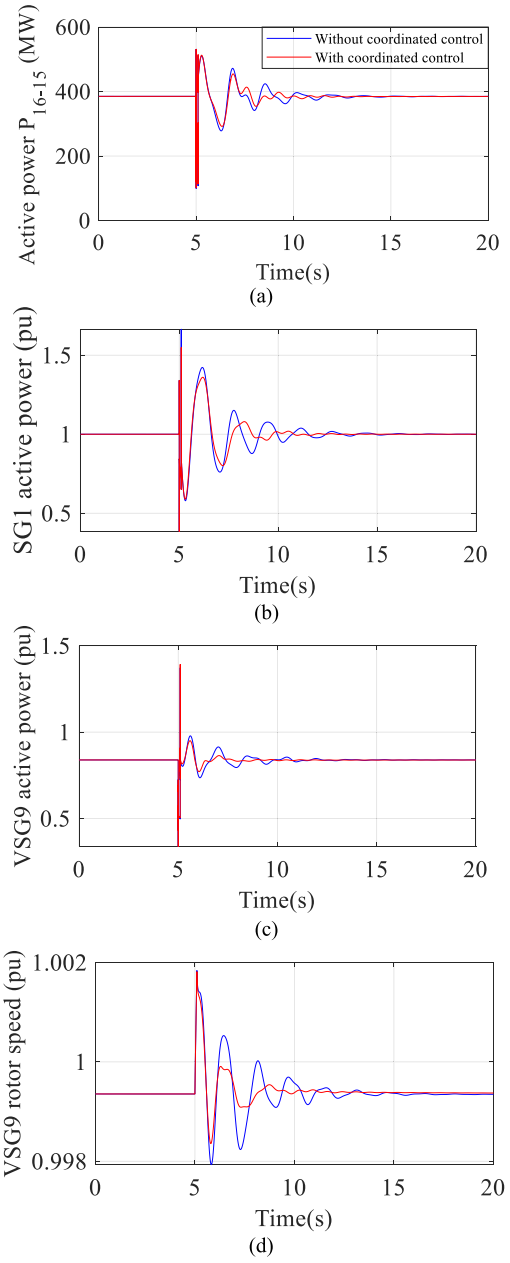

FIGURE 21. **39-bus system response under fault disturbance.**

and active power of VSG9 are selected to observe the system response. The simulation results are shown in Fig. 19.

2) LOAD DISTURBANCE

In this case, an additional 200 MW load is suddenly added at Bus 16. The same signals as part 1) are shown in Fig. 20 to observe the effects of the designed controller.

3) THREE-PHASE-TO-GROUND-FAULT DISTURBANCE

A three-phase-to-ground fault is simulated for this case, it occurs at Bus 3 with a duration of 0.1s. Similarly, the simulation results of the same selected signals in previous parts are illustrated in Fig. 21.

From Fig. 19 to Fig. 21, it can be seen that the designed controller can suppress the oscillation of VSG9 effectively. Meanwhile, the oscillation amplitude of the power flow on line 15-16 can be alleviated as well. It can also provide damping support to the rotor speed of SG1.

VI. CONCLUSION

This paper has investigated the impact of multiple VSGs on power system low frequency oscillations. From the modal analysis, it has been found that the VSGs are participating in the low frequency oscillation modes and have strong

interactions with traditional synchronous generators. Then a coordinated decentralized sequential design approach for supplementary damping controller for multiple VSGs has been proposed using measurement-based Prony analysis which aims to obtain the oscillation modes of the system, and the advantages of such method is that it facilitates the mode extraction where it is not possible to get the detailed structural model of targeted system. This feature is particularly useful for large scale power system applications and controller designs. The proposed approach has been demonstrated on the modified two-area 11-bus system and the 39-bus system, which verify the effectiveness of the designed controllers.

APPENDIX

TABLE 3. VSG controller parameters [24], [31].

D_p.	20 pu	D_q	10 pu
K_d	35 pu	K	5 pu
H	7 s	R_v	0.1 pu
L_v	0.3		

REFERENCES

[1] M. S. Alam, F. S. Al-Ismail, A. Salem, and M. A. Abido, "High-level penetration of renewable energy sources into grid utility: Challenges and solutions," *IEEE Access*, vol. 8, pp. 190277–190299, 2020.

[2] Q.-C. Zhong and G. Weiss, "Synchronverters: Inverters that mimic synchronous generators," *IEEE Trans. Ind. Electron.*, vol. 58, no. 4, pp. 1259–1267, Apr. 2011.

[3] L. Zhang, L. Harnefors, and H.-P. Nee, "Interconnection of two very weak AC systems by VSC-HVDC links using power-synchronization control," *IEEE Trans. Power Syst.*, vol. 26, no. 1, pp. 344–355, Feb. 2011.

[4] J. Zhu, C. D. Booth, G. P. Adam, A. J. Roscoe, and C. G. Bright, "Inertia emulation control strategy for VSC-HVDC transmission systems," *IEEE Trans. Power Syst.*, vol. 28, no. 2, pp. 1277–1287, May 2013.

[5] S. D'Arco, J. A. Suul, and O. B. Fosso, "A virtual synchronous machine implementation for distributed control of power converters in smartgrids," *Electr. Power Syst. Res.*, vol. 122, pp. 180–197, May 2015.

[6] J. Liu, Y. Miura, and T. Ise, "Fixed-parameter damping methods of virtual synchronous generator control using state feedback," *IEEE Access*, vol. 7, pp. 99177–99190, 2019.

[7] B. Tian, X. Mo, Y. Shen, W. Lei, and P. Xu, "Prospect and key techniques of global energy interconnection Zhangjiakou innovation demonstration zone," *Global Energy Interconnection*, vol. 1, no. 2, pp. 153–161, 2018.

[8] M. Li, Y. Wang, Y. Liu, N. Xu, S. Shu, and W. Lei, "Enhanced power decoupling strategy for virtual synchronous generator," *IEEE Access*, vol. 8, pp. 73601–73613, 2020.

[9] H. Xu, C. Yu, C. Liu, Q. Wang, and X. Zhang, "An improved virtual inertia algorithm of virtual synchronous generator," *J. Mod. Power Syst. Clean Energy*, vol. 8, no. 2, pp. 377–386, 2020.

[10] T. Shintai, Y. Miura, and T. Ise, "Oscillation damping of a distributed generator using a virtual synchronous generator," *IEEE Trans. Power Del.*, vol. 29, no. 2, pp. 668–676, Apr. 2014.

[11] J. Chen, M. Liu, F. Milano, and T. O'Donnell, "100% converter-interfaced generation using virtual synchronous generator control: A case study based on the Irish system," *Electr. Power Syst. Res.*, vol. 187, Oct. 2020, Art. no. 106475.

[12] K. Shi, W. Song, H. Ge, P. Xu, Y. Yang, and F. Blaabjerg, "Transient analysis of microgrids with parallel synchronous generators and virtual synchronous generators," *IEEE Trans. Energy Convers.*, vol. 35, no. 1, pp. 95–105, Mar. 2020.

[13] Y. Hirase, K. Sugimoto, K. Sakimoto, and T. Ise, "Analysis of resonance in microgrids and effects of system frequency stabilization using a virtual synchronous generator," *IEEE J. Emerg. Sel. Topics Power Electron.*, vol. 4, no. 4, pp. 1287–1298, Dec. 2016.

[14] L. Huang, H. Xin, and Z. Wang, "Damping low-frequency oscillations through VSC-HVDC stations operated as virtual synchronous machines," *IEEE Trans. Power Electron.*, vol. 34, no. 6, pp. 5803–5818, Jun. 2019.

[15] J. Alipoor, Y. Miura, and T. Ise, "Power system stabilization using virtual synchronous generator with alternating moment of inertia," *IEEE J. Emerg. Sel. Topics Power Electron.*, vol. 3, no. 2, pp. 451–458, Jun. 2015.

[16] C. Cheng, Z. Zeng, H. Yang, and R. Zhao, "Wireless parallel control of three-phase inverters based on virtual synchronous generator theory," in *Proc. Int. Conf. Electr. Mach. Syst. (ICEMS)*, Oct. 2013, pp. 162–166.

[17] B. Gao, C. Xia, N. Chen, K. Cheema, L. Yang, and C. Li, "Virtual synchronous generator based auxiliary damping control design for the power system with renewable generation," *Energies*, vol. 10, no. 8, p. 1146, Aug. 2017.

[18] Z. Shuai, W. Huang, Z. J. Shen, A. Luo, and Z. Tian, "Active power oscillation and suppression techniques between two parallel synchronverters during load fluctuations," *IEEE Trans. Power Electron.*, vol. 345, no. 4, pp. 4127–4142, Apr. 2019.

[19] S. Dawei, L. Hui, S. Peng, G. Shunan, and S. Yamin, "Stability analysis of photovoltaic virtual synchronous generators," in *Proc. China Int. Conf. Electr. Distrib. (CICED)*, Sep. 2018, pp. 1938–1944.

[20] J. Chen and T. O'Donnell, "Parameter constraints for virtual synchronous generator considering stability," *IEEE Trans. Power Syst.*, vol. 34, no. 3, pp. 2479–2481, May 2019.

[21] M. Ebrahimi, S. A. Khajehoddin, and M. Karimi-Ghartemani, "An improved damping method for virtual synchronous machines," *IEEE Trans. Sustain. Energy*, vol. 10, no. 3, pp. 1491–1500, Jul. 2019.

[22] J. Liu, Y. Miura, H. Bevrani, and T. Ise, "Enhanced virtual synchronous generator control for parallel inverters in microgrids," *IEEE Trans. Smart Grid*, vol. 8, no. 5, pp. 2268–2277, Sep. 2017.

[23] J. M. Mauricio and A. E. Leon, "Improving small-signal stability of power systems with significant converter-interfaced generation," *IEEE Trans. Power Syst.*, vol. 35, no. 4, pp. 2904–2914, Jul. 2020.

[24] M. Chen, D. Zhou, and F. Blaabjerg, "Active power oscillation damping based on acceleration control in paralleled virtual synchronous generators system," *IEEE Trans. Power Electron.*, vol. 36, no. 8, pp. 9501–9510, Aug. 2021.

[25] H. Ye, W. Pei, L. Kong, and T. An, "Low-order response modeling for wind farm-MTDC participating in primary frequency controls," *IEEE Trans. Power Syst.*, vol. 34, no. 2, pp. 942–952, Mar. 2019.

[26] M. Baruwa and M. Fazeli, "Impact of virtual synchronous machines on low-frequency oscillations in power systems," *IEEE Trans. Power Syst.*, vol. 36, no. 3, pp. 1934–1946, May 2021.

[27] M. Mao, C. Qian, and Y. Ding, "Decentralized coordination power control for islanding microgrid based on PV/BES-VSG," *CPSS Trans. Power Electron. Appl.*, vol. 3, no. 1, pp. 14–24, Mar. 2018.

[28] S. Adhikari, Q. Xu, Y. Tang, P. Wang, and X. Li, "Decentralized control of two DC microgrids interconnected with tie-line," *J. Mod. Power Syst. Clean Energy*, vol. 5, no. 4, pp. 599–608, Jul. 2017.

[29] J. Deng, C. Li, and X. P. Zhang, "Coordinated design of multiple robust FACTS damping controllers: A BMI-based sequential approach with multi-model systems," *IEEE Trans. Power Syst.*, vol. 30, no. 6, pp. 3150–3159, Nov. 2015.

[30] D. J. Trudnowski, J. R. Smith, T. A. Short, and D. A. Pierre, "An application of Prony methods in PSS design for multimachine systems," *IEEE Trans. Power Syst.*, vol. 6, no. 1, pp. 118–126, Feb. 1991.

[31] D. Pan, X. Wang, F. Liu, and R. Shi, "Transient stability of voltage-source converters with grid-forming control: A design-oriented study," *IEEE J. Emerg. Sel. Topics Power Electron.*, vol. 8, no. 2, pp. 1019–1033, Jun. 2020.

[32] W. Zhang, A. M. Cantarellas, J. Rocabert, A. Luna, and P. Rodriguez, "Synchronous power controller with flexible droop characteristics for renewable power generation systems," *IEEE Trans. Sustain. Energy*, vol. 7, no. 4, pp. 1572–1582, Oct. 2016.

[33] H. Xin, L. Huang, L. Zhang, Z. Wang, and J. Hu, "Synchronous instability mechanism of P-f droop-controlled voltage source converter caused by current saturation," *IEEE Trans. Power Syst.*, vol. 31, no. 6, pp. 5206–5207, Nov. 2016.

[34] I. Abdulrahman, "MATLAB-based programs for power system dynamic analysis," *IEEE Open Access J. Power Energy*, vol. 7, pp. 59–69, 2020.

[35] P. Kundur, N. J. Balu, and M. G. Lauby, *Power System Stability and Control*. New York, NY, USA: McGraw-Hill, 1994.

[36] H. T. Nguyen, G. Yang, A. H. Nielsen, P. H. Jensen, and B. Pal, "Applying synchronous condenser for damping provision in converter-dominated power system," *J. Mod. Power Syst. Clean Energy*, vol. 9, no. 3, pp. 639–647, Sep. 2020.
[37] M. Edrah *et al.*, "Effects of POD control on a DFIG wind turbine structural system," *IEEE Trans. Energy Convers.*, vol. 35, no. 2, pp. 765–774, Jun. 2020.
[38] M. Pai, *Energy Function Analysis for Power System Stability*. New York, NY, USA: Springer, 2012.

MIN ZHAO received the joint B.E. degree from Huazhong University of Science and Technology, Wuhan, China, and the University of Birmingham, Birmingham, U.K., in 2016, where he is currently pursuing the Ph.D. degree.

HANG YIN received the Ph.D. degree from the Power Electronics Group, TU Berlin, Germany. He is currently a Senior Researcher and the Director Assistant of the Innovative Energy Technology Department, Global Energy Interconnection Research Institute Europe (GEIRI Europe), State Grid Corporation of China. In August 2014, he joined GEIRI Europe. He is currently leading several projects, e.g., Coordinate Control of Multiple Virtual Synchronous Generators for Power System. His main research interests include power converter control for renewable energy integration and HVDC systems.

YING XUE (Senior Member, IEEE) received the joint B.E. degree in electrical engineering from Huazhong University of Science and Technology (HUST), Wuhan, China, and the University of Birmingham, Birmingham, U.K., in 2012, and the Ph.D. degree in electrical engineering from the University of Birmingham in 2016. He is currently a Lecturer at the University of Birmingham. His main research area is HVDC modeling and control.

XIAO-PING ZHANG (Fellow, IEEE) is currently a Professor of electrical power systems with the University of Birmingham, U.K., and also the Director of smart grid at Birmingham Energy Institute and the Co-Director of Birmingham Energy Storage Center. He coauthored the first and second edition of the monograph *Flexible AC Transmission Systems: Modeling and Control* (Springer, 2006 and 2012). He also coauthored the book *Restructured Electric Power Systems: Analysis of Electricity Markets with Equilibrium Models* (IEEE Press/Wiley, 2010). He has been the Advisor to IEEE PES UK & Ireland Chapter and chairing the IEEE PES WG on Test Systems for Economic Analysis. He has been appointed recently to the Expert Advisory Group of U.K. Government's Offshore Transmission Network Review. His research interests include modeling and control of HVDC, FACTS, and wind/wave generation, distributed energy systems and market operations, and power system planning. He has been made a fellow of IEEE for his contributions to modeling and control of high-voltage DC and AC transmission systems. He is an IEEE PES Distinguished Lecturer on HVDC, FACTS, and wave energy generation. He is also a fellow of IET.

YUANLIANG LAN received the B.S. and M.S. degrees in electrical engineering from Northeast China Electrical Power Institute, Jilin, China, in 1994 and 1997, respectively, and the Ph.D. degree from China Electrical Power Research Institute (CEPRI), Beijing, China, in 2006. He is currently the Chief Engineer of the CPS-ISM Group, GEIRI EU. His research interests include renewable energy integration, FACTS and HVDC, and intelligent power electronics.